AE International – Europe

Atmospheric Environment 38 (2004) 6211–6222

ATMOSPHERIC ENVIRONMENT

www.elsevier.com/locate/atmosenv

Modelling ozone fluxes over Hungary

István Lagzi[a,*], Róbert Mészáros[b], László Horváth[c], Alison Tomlin[d], Tamás Weidinger[b], Tamás Turányi[a], Ferenc Ács[b], László Haszpra[c]

[a]*Department of Physical Chemistry, Eötvös Loránd University, Pázmány P. stny 1.A, P.O. Box 32, H-1518 Budapest, Hungary*
[b]*Department of Meteorology, Eötvös Loránd University, P.O. Box 32, H-1518 Budapest, Hungary*
[c]*Hungarian Meteorological Service, P.O. Box 39, H-1675 Budapest, Hungary*
[d]*Department of Fuel and Energy, University of Leeds, Leeds, LS2 9JT, UK*

Received 26 January 2004; received in revised form 25 June 2004; accepted 12 July 2004

Abstract

This paper presents and utilises a coupled Eulerian photochemical reaction–transport model and a detailed ozone dry-deposition model for the investigation of ozone fluxes over Hungary. The reaction–diffusion–advection equations relating to ozone formation, transport and deposition are solved on an unstructured triangular grid using the SPRINT2D code. The model domain covers Central Europe including Hungary, which is located at the centre of the domain and is covered by a high-resolution nested grid. The sophisticated dry-deposition model estimates the dry-deposition velocity of ozone by calculating the aerodynamic, the quasi-laminar boundary layer and the canopy resistance. The meteorological data utilised in the model were generated by the ALADIN meso-scale limited area numerical weather prediction model used by the Hungarian Meteorological Service. The ozone fluxes were simulated for three soil wetness states, corresponding to wet, moderate and dry conditions. The work demonstrates that the spatial distribution of ozone concentration is a less accurate measure of effective ozone load, than the spatial distribution of ozone fluxes. The fluxes obtained show characteristic spatial patterns, which depend on the soil wetness, the meteorological conditions, the ozone concentration and the underlying land use.

Keywords: Dry-deposition model; Photochemical air pollution model; Ozone; Soil wetness conditions; Stomatal fluxes

1. Introduction

The phytotoxic nature of ozone has been known for decades (for a review see Krupa and Manning, 1988). Because of high emissions of ozone precursor substances, elevated ozone concentrations may cover large areas in Europe for both shorter episodes or longer periods (Hjellbrekke and Solberg, 2002) under certain meteorological conditions. These elevated concentrations can be potentially damaging to agricultural and natural vegetation. Occasional extreme concentrations may cause visible injury to the vegetation while the long-term, growing season averaged exposure can result in decreased productivity and crop yield (Fuhrer et al., 1997). This characteristic has led to the development of the accumulated exposure over a threshold (AOT) concept through a series of UN-ECE workshops (Fuhrer et al., 1997). Based on experimental data,

*Corresponding author. Tel.: +36-2090555; fax: +36-12090602.
E-mail address: lagzi@vuk.chem.elte.hu (I. Lagzi).

1352-2310/$ - see front matter © 2004 Elsevier Ltd. All rights reserved.
doi:10.1016/j.atmosenv.2004.07.018

40 ppb was accepted as the threshold (AOT40) below which significant damage was unlikely (Kärenlampi and Skärby, 1996). This concept was accepted by the UN-ECE convention on long-range transboundary air pollution (LRTAP) and by the new directive of European Union (2002/3/EC) relating to ozone in ambient air.

It was already clear in the development phase of the AOT concept that there was no direct relationship between the AOT values and the actual vegetation damage, crop loss, etc. (Fuhrer et al., 1997). Since ozone enters the plant through the stomata, the plant response is more closely related to the ozone flux than to atmospheric concentrations. The damage depends not only on the plant species, but also on its growing phase and the environmental conditions that influence the ozone transfer from the atmosphere into the plant (Sofiev and Tuovinen, 2001). Application of a universal AOT40 critical level may drive countries with less sensitive vegetation into economically undue environmental investments (De Santis, 1999).

The threshold value of 40 ppb is rather close to the mean ozone-mixing ratio. Consequently, any uncertainty, or imprecision of monitored values may cause significant bias in the calculated AOT40 values. Because of the strong gradient in the ozone-mixing ratio close to the surface, the sampling elevation is also critical (Tuovinen, 2000). The spatial coverage of the ozone-monitoring network has improved in recent years, and approaches an acceptable level in Northern Europe and parts of Central Europe. However, the network is still fairly sparse in the eastern and southern regions of the continent, implying that the use of measurements alone gives a snapshot of concentration gradients, and potentially fluxes, but does not allow the study of fluxes across a wide range of land use conditions, particularly in regions of steep ozone concentration gradients. Hungary also belongs to the poorly covered region of Europe where there is only one ozone-monitoring station reporting data to the international databases.

Taking into account the above weaknesses and considering the advantages of contemporary micrometeorological measuring techniques, there is a potential advantage in directly measuring or modelling the ozone deposition onto the surface and therefore the ozone flux into the plants. Such measures may be more closely related to plant damage and therefore economical losses and as such might be a more appropriate basis for future regulations (e.g. Emberson et al., 2000a). Because of the lack of spatial coverage of available monitoring equipment, the development of an appropriate computational tool for modelling ozone fluxes is desirable.

In this paper high spatial resolution ozone flux calculations are presented using an Eulerian chemical–transport model which includes chemical reactions, transport and deposition processes. The calculated pollutant concentrations have spatial resolution higher than those obtained from former calculations based on simulations with EMEP (Jonson et al., 2001) and Danish Eulerian model (DEM) (Havasi and Zlatev, 2002). As an illustration, the performance of the model is demonstrated for conditions that occurred in Hungary during 22–23 July 1998, when elevated ozone concentration covered the whole Carpathian Basin.

2. The dispersion–deposition model

In order to achieve a detailed parameterisation of ozone fluxes over Hungary, a high resolution dispersion and a dry-deposition model have been coupled. The structure of the model calculations is shown in Fig. 1. Descriptions of the two models are presented in the following subsections.

2.1. The dry-deposition model

Models for estimating the dry deposition of ozone are based on the so-called inferential method (Baldocchi et al., 1987; Hicks et al., 1987; Padro et al., 1991, 1998; Kramm et al., 1995; Padro 1996; Walmsley and Wesely, 1996; Grünhage and Haenel, 1997; Meyers et al., 1998; Brook et al., 1999; Emberson et al., 2000b; Klemm and Mangold, 2001; Zhang et al., 2002). In these models the ozone deposition velocity is estimated as the reciprocal of the resistance. The models differ from each other in terms of their input data and resistance parameterisations. According to Zhang et al. (2001), the accuracy of the calculations is not in direct correlation with the complexity of the models, since there are uncertainties in the chemical, physical and biological processes governing the ozone flux. In contrast to complex, multi-layer models, which contain significant uncertainties, single-layer models or big-leaf models have been developed. These models require less input data and are therefore thought to be more suitable for operational modelling (e.g. Grünhage and Haenel, 1997; Emberson et al., 2000b; Zhang et al., 2002).

This paper reports the development of a single-layer dry-deposition model for Hungary, for continental climatic conditions characterised by hot and dry summers. The dry-deposition velocity and the ozone flux can be estimated at any arbitrary point and time over different types of vegetation (grass, agricultural field, orchard, coniferous, deciduous and mixed forest), bare soil, urban area, water and snow-covered surface. The land-cover map was generated based on a Hungarian land-use map. For each grid cell the dominant surface type was chosen.

The dry-deposition model was applied on the grid of the meso-scale limited area numerical weather prediction model ALADIN (Horányi et al., 1996). The time and

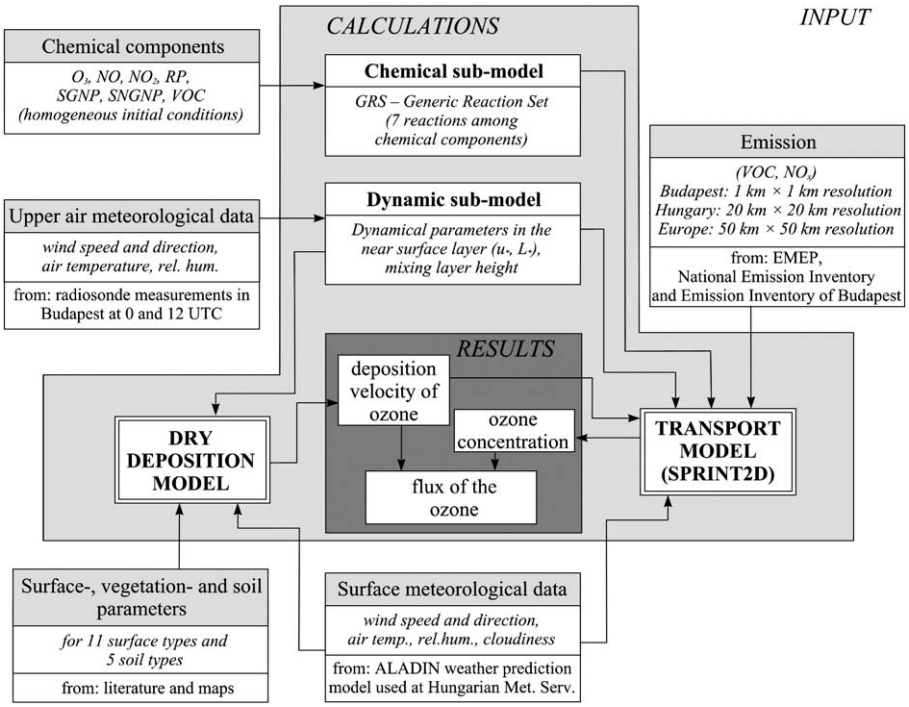

Fig. 1. The flowchart of the coupled dispersion–deposition model.

space resolution of the data is 6 h and 0.10×0.15 deg (approximately $11\,\text{km} \times 11\,\text{km}$), respectively. In these runs the atmospheric forcing data (air temperature, relative humidity, wind speed, air pressure and cloudiness) obtained by the ALADIN model are used.

The deposition velocity (v_d) is defined as the inverse of the sum of the atmospheric and surface resistances, which retards the ozone flux:

$$v_d = (R_a + R_b + R_c)^{-1}, \tag{1}$$

where R_a, R_b and R_c are the aerodynamic resistance, the quasi-laminar boundary layer resistance and the canopy resistance, respectively. Each resistance is parameterised as simply as possible but not at the cost of accuracy.

The aerodynamic resistance is calculated using Monin–Obukhov's similarity theory, taking into account the atmospheric stability (Ács and Szász, 2002). The boundary layer resistance is calculated by an empirical relationship (Hicks et al., 1987). The canopy resistance R_c is parameterised by equation

$$R_c = \frac{1}{(R_{st} + R_{mes})^{-1} + (R_s)^{-1} + (R_{cut})^{-1}}, \tag{2}$$

where R_{st}, R_{mes}, R_s and R_{cut} are the stomatal, mesophyll, surface and cuticular resistances, respectively. The mesophyll resistance for ozone in the model is taken as $R_{mes} = 0$. Cuticular resistance, R_{cut}, and surface resistance, R_s, for ozone deposition were obtained from the literature (Table 1).

Stomatal resistance of an individual leaf, r_{st}, can be calculated from the empirical formula of Jarvis (1976) knowing soil and plant physiological characteristics:

$$r_{st} = \frac{r_{st,min}\left(1 + b_{st}/\text{PAR}\right)}{f_t(t) f_e(e) f_\theta(\theta) f_{D,i}}, \tag{3}$$

where $r_{st,min}$ is the minimum stomatal resistance for water vapour, b_{st} is a plant species-dependent constant and PAR is the photosynthetically active radiation. The factors in the denominator range between 0 and 1, and modify the stomatal resistance, $f_t(t)$, $f_e(e)$ and $f_\theta(\theta)$ describe the effect of temperature, the vapour pressure deficit and plant water stress on stomata, while $f_{D,i}$ modifies the stomatal resistance for the pollutant gas of interest (for ozone, $f_{D,i} = 0.625$ after Wesely (1989)).

Jarvis' formula referring to a vegetation canopy is

$$R_{st} = \frac{1}{G_{st}(PAR) f_t(t) f_e(e) f_\theta(\theta) f_{D,i}}, \tag{4}$$

where $G_{st}(\text{PAR})$ is the unstressed canopy stomatal conductance, a function of PAR. This term is estimated

Table 1
Vegetation-specific parameters used in the dry-deposition model

Parameter	Land use category				
	Grassland[a]	Agricultural land[b]	Orchard, vineyard[c]	Deciduous forest[d]	Mixed forest[d]
$r_{st,min}$ ($s\,m^{-1}$)	50	125	130	150	200
R_{cut} ($s\,m^{-1}$)	2000	2000	4000	2000	2000
R_{soil} ($s\,m^{-1}$)	300	300	550	300	300
b_{st} ($W\,m^{-2}$)	20	45	30	43	44
LAI ($m^2\,m^{-2}$)	2	2	3	3.4	4.5

[a] *Sources:* Meyers et al. (1998), Brook et al. (1999), Zhang et al. (2002).
[b] *Sources:* Baldocchi et al. (1987), Hicks et al. (1987), Meyers et al. (1998), Brook et al. (1999).
[c] *Sources:* Padro (1996), Zhang et al. (1996), Brook et al. (1999).
[d] *Sources:* Brook et al. (1999).

by Zhang et al. (2001). In this parameterisation, the canopy is divided into sunlit leaves and shaded leaves, and G_{st} is calculated with the following form

$$G_{st}(\mathrm{PAR}) = \frac{\mathrm{LAI_s}}{r_{st}(\mathrm{PAR_s})} + \frac{\mathrm{LAI_{sh}}}{r_{st}(\mathrm{PAR_{sh}})}, \quad (5)$$

$$r_{st}(\mathrm{PAR}) = r_{st,min}\left(1 + b_{st}/\mathrm{PAR}\right), \quad (6)$$

where $\mathrm{LAI_s}$ and $\mathrm{LAI_{sh}}$ are the total sunlit and shaded leaf area indexes, respectively, and $\mathrm{PAR_s}$ and $\mathrm{PAR_{sh}}$ are PAR received by sunlit and shaded leaves, respectively.

$\mathrm{LAI_s}$, $\mathrm{LAI_{sh}}$, $\mathrm{PAR_s}$ and $\mathrm{PAR_{sh}}$ terms are parameterised by Zhang et al. (2001). The vegetation-specific terms $r_{st,min}$, b_{st} and LAI are presented in Table 1.

The dimensionless functions $f_t(t)$ and $f_e(e)$ in Eq. (4) are the same as used in Brook et al. (1999). The water stress function $f_\theta(\theta)$ is parameterised using soil water content (θ):

$$f_\theta = \begin{cases} 1 & \text{if } \theta > \theta_f \\ \max\left\{\frac{\theta-\theta_w}{\theta_f-\theta_w},\ 0.05\right\} & \text{if } \theta_w < \theta \leqslant \theta_f \\ 0.05 & \text{if } \theta \leqslant \theta_w \end{cases}, \quad (7)$$

where θ_w and θ_f are the wilting point and the field capacity soil moisture contents, respectively. These terms depend on the soil texture of the grid cell. The soil texture was determined by Várallyay et al. (1980). The grid cell soil texture is represented by the dominant soil texture. The θ_w and θ_f values for several soil textures are provided in Table 2 using data from Ács (2003). In Hungary, under continental climate conditions, deposition is frequently obstructed by soil water deficiency. Soil water content, θ, can be modelled by a simple bucket model (Mintz and Walker, 1993). However, in this application θ is prescribed. Three θ-values are used which represent two extreme (a dry and a wet conditions) and a moderate wetness conditions. In the dry case $\theta = \theta_w$, while in the wet case $\theta = \theta_f$. For moderate wetness condition $\theta = (\theta_w + \theta_f)/2$.

Table 2
Hungarian soil characteristics

Soil texture	Wilting point soil moisture content θ_w ($m^3\,m^{-3}$)	Field capacity soil moisture content θ_f ($m^3\,m^{-3}$)
Sand	0.03	0.15
Sandy loam	0.11	0.29
Loam	0.14	0.33
Clay loam	0.18	0.36
Clay	0.25	0.41

2.2. The dispersion model

The horizontal dispersion of species is described within an unstructured triangular Eulerian grid framework (Lagzi et al., 2001, 2002). The modelled area is a 980 km × 920 km region of Central Europe with Hungary at the centre. The atmospheric transport–reaction–diffusion equation is the following in two space dimensions:

$$\frac{\partial c_s}{\partial t} = -\frac{\partial(uc_s)}{\partial x} - \frac{\partial(vc_s)}{\partial y} + \frac{\partial}{\partial x}\left(K_x\frac{\partial c_s}{\partial x}\right) + \frac{\partial}{\partial y}\left(K_y\frac{\partial c_s}{\partial y}\right) + R_s(c_1, c_2, \ldots, c_n) + E_s - k_s c_s, \quad (8)$$

where c_s is the concentration of the sth compound, u and v are the horizontal wind speeds, K_x and K_y are the eddy diffusivity coefficients and k_s is the dry-deposition rate constant. E_s describes the distribution of the emission sources for the sth compound and R_s is the chemical

reaction term, which may contain non-linear terms in c_s. For n chemical species, an n-dimensional set of partial differential equations is formed describing the rates of change of species concentrations over time and space, and these concentrations are coupled through the non-linear chemical reaction term (Tomlin et al., 1997; Hart et al., 1998).

The four vertical layers of the model are the surface layer (extending to 50 m), the mixing layer, the reservoir layer and the free troposphere layer. At night, the mixing layer extends to the height determined by the midnight radiosonde data. During the day, the height of the mixing layer is assumed to rise smoothly from sunrise to the height determined by the noon radiosonde measurement. In the evening, it goes back to the night-time level. The reservoir layer extends from the top of the mixing layer to an altitude of 1000 m. This layer may vanish if the mixing height exceeds the top of the reservoir layer. The vertical mixing of pollutants is approximated by a parameterised description of mixing between the layers. This is achieved by parameterisation of the vertical eddy diffusion between the surface and mixing layers, and fumigation between the mixing layer, and either the reservoir or upper layer above it. The eddy diffusivity coefficients for the x and y directions were set to $50\,m^2\,s^{-1}$ for all species (Van Loon, 1996). Detailed description of the vertical eddy diffusivity is presented by Lagzi et al. (2004). The local wind speed and direction, relative humidity, temperature and cloud coverage were determined by the meteorological model ALADIN for each of the four layers. Meteorological data and the dry-deposition velocity of ozone were interpolated in order to obtain data relevant to a given point in space on the unstructured grid using mass conservative methods.

For Budapest, a $1\,km \times 1\,km$ spatial resolution emission inventory was applied, which included the most significant 63 emission point sources for NO_x and VOCs. For Hungary, the National Emission Inventory of spatial resolution $20\,km \times 20\,km$ was used, which contains both area and point sources. Outside Hungary, the emission inventories of EMEP for NO_x and VOCs were used, having a spatial resolution of $50\,km \times 50\,km$. In the present simulations, the Gereric Reaction Set (GRS) chemical scheme (Azzi et al., 1992) was used.

The system of the partial differential equations is discretised using a finite volume, method of lines based approach (Tomlin et al., 1997) and integrated in time using code SPRINT2D with a variable time-step method (Berzins et al., 1989; Berzins and Ware, 1995). Operator splitting is carried out at the level of the non-linear equations by approximating the Jacobian matrix. Further details of the method are presented in Tomlin et al. (1997).

3. Results and discussion

The simulated period was from noon 22 July to midnight 23 July, 1998. This period was chosen because during the selected days, the high temperature, low cloud cover and low wind speed resulted in high photooxidant levels in Hungary. Three simulations, corresponding to three different soil wetness conditions (dry, wet and moderate), were carried out.

The grid structure during the simulations included a fixed fine nested grid over Hungary, which had an edge size of 12.5 km and a coarse grid outside of the rectangle covering Hungary as shown in Fig. 2. This coarser grid was characterised by an edge length of 100 km. The initial concentrations of the major species were 0.4 ppb for NO_2, 2.0 ppb for NO, 80 ppb for O_3, and 4.1 ppb for VOC, which correspond to typical daytime species concentrations. The initial concentrations were equal in each layer across the whole simulated domain.

The simulated and measured ozone concentrations at the K-puszta monitoring station of the Hungarian Meteorological Service located about 80 km south of Budapest (46°58′N, 19°33′E, 125 m a.s.l.) are shown in Fig. 3. The three simulated concentration data series that correspond to the three assumed soil wetness states are in accordance with the measured ones. According to the results, the simulated ozone concentration practically does not depend on soil wetness conditions since the greatest difference between the calculated data for the three specified conditions is not higher than 5%. These differences are higher during the daytime, but lower in the night-time. In some cases the transport model overestimated the measured ozone concentration. No trivial source of these discrepancies has been found, but these may be caused by uncertainties in the emisson statistics, atmospheric data and also the local effects around the monitoring station.

The simulated spatial distribution of ozone concentrations at 00 and 12 UTC on 23 July 1998 are shown in Fig. 4. Distribution of the deposition velocities and the ozone fluxes at 00 UTC and for three different soil wetness states (dry, moderately wet and wet) at 12 UTC on 23 July 1998 are presented in Figs. 5–8, respectively. Additionally, for cases corresponding to moderately wet and wet conditions, stomatal fluxes of ozone are also plotted in Figs. 7 and 8, respectively.

Calculated deposition velocities of ozone over different vegetation types were compared with observations based on data from the literature (Table 3). The modelled data are in good agreement with observed ones.

The deposition velocity is low at night-time, because stratification of the near surface layer is stable, and the turbulence is weak. At this time, the ozone flux is mainly controlled by the concentration of ozone, although this

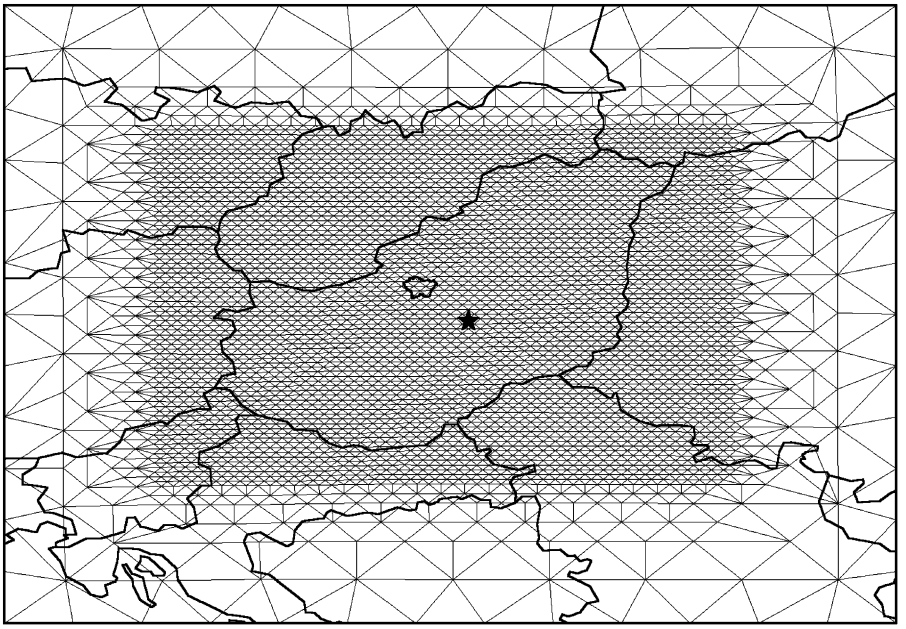

Fig. 2. The grid structure of the dispersion model. The average mesh length of the outer coarse and that of the nested fine grid are 100 and 12.5 km, respectively. The asterisk indicates the location of the K-puszta EMEP monitoring station of the Hungarian Meteorological Service.

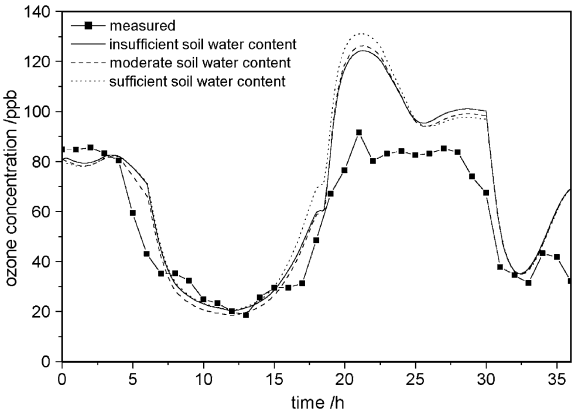

Fig. 3. Comparison of the calculated ozone concentrations at three different soil water contents with the measured ozone concentrations at the K-puszta monitoring stations. Simulation started at 22 July 1998 at 12 UTC.

is low compared with the daytime values due to the lack of photolysis. The impact of soil wetness on the ozone flux via stomatal regulation is negligible at night-time and therefore only results related to moderate soil water content are shown in Fig. 5. The reason for this is that the model assumed that the stomata are closed in the absence of insolation and therefore deposition through the stomata is obstructed.

In contrast, during the daytime, when stomatal transfer plays an important role in the total deposition, the deposition velocity and ozone fluxes are strongly dependent on the soil water content (see Figs. 6–8). Because of stronger turbulent motions in the surface layer, the deposition velocity in the daytime is one order of magnitude greater than during the night-time, unless insufficient soil water content blocks the deposition. The ozone fluxes for a particular location can therefore vary significantly for different soil water contents under the same background atmospheric conditions and local ozone concentrations, as shown in Figs. 6–8. Soil wetness condition also has a great impact on the ratio of the stomatal part of ozone fluxes. In the case of moderate soil wetness conditions, the ratio of stomatal and total fluxes ranged between 22% and 68% (Fig. 7). The same ratio for sufficient soil water content varied between 22% and 78% (Fig. 8). Low per cents of the stomotal fluxes are due to the high vapour pressure deficit, which also diminishes the transfer through the stomata. For cases where there is insufficient soil water content, the stomatal transfer is blocked in the model, and as a consequence, ozone is deposited mostly via other pathways. For low soil water content a small

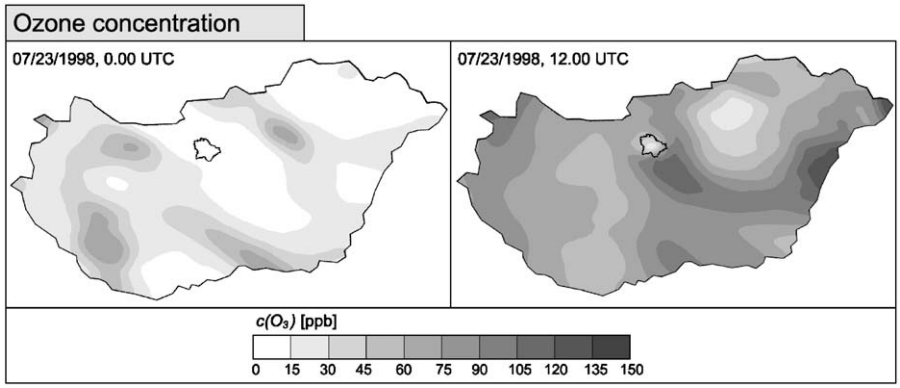

Fig. 4. Calculated ozone concentration on 23 July 1998 at 00 and 12 UTC. Results correspond to moderate soil wetness conditions.

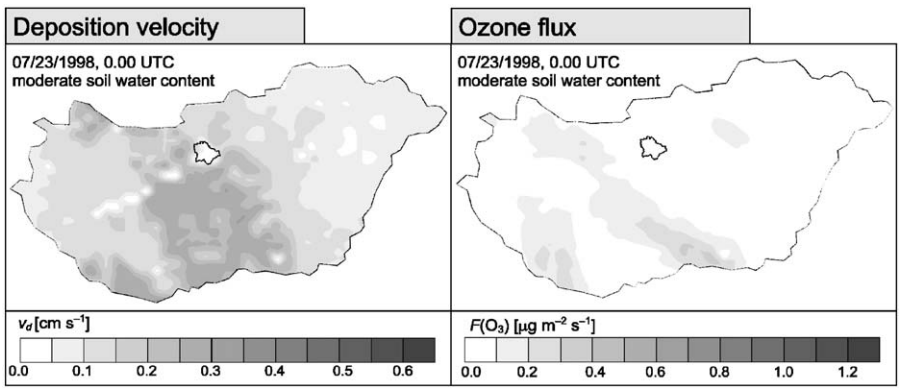

Fig. 5. Calculated dry-deposition velocity and flux of ozone on 23 July 1998 at 00 UTC. Results correspond to moderate soil wetness conditions.

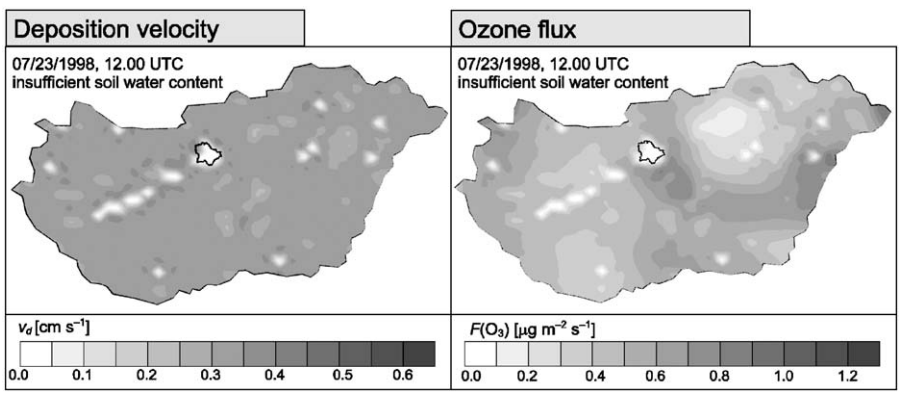

Fig. 6. Calculated dry-deposition velocity and flux of ozone on 23 July 1998 at 12 UTC. Results correspond to insufficient soil wetness conditions.

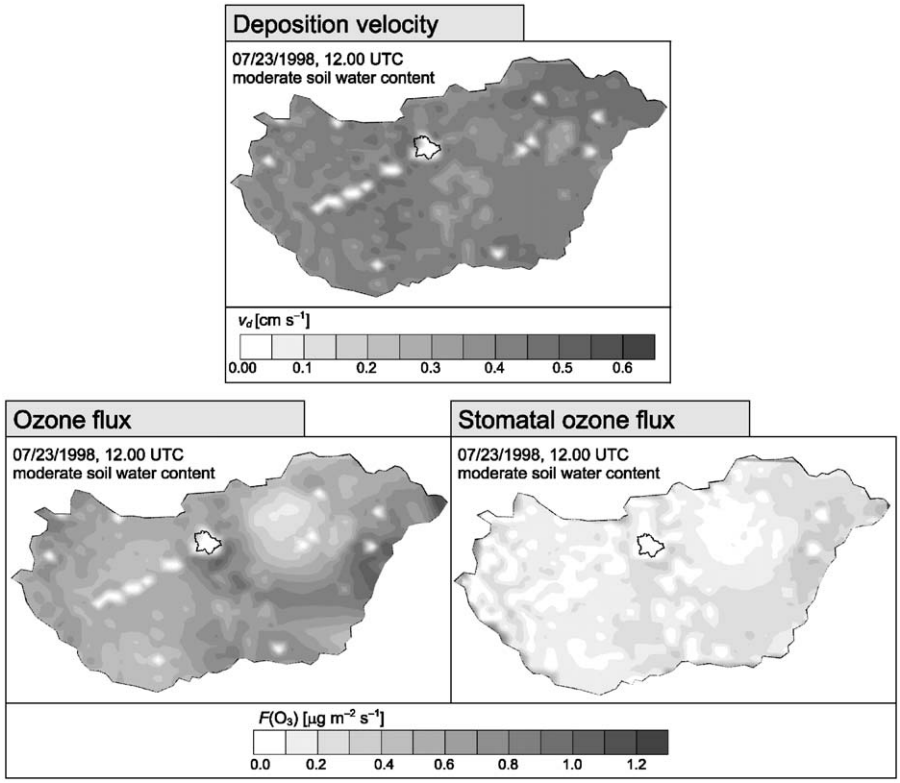

Fig. 7. Calculated dry-deposition velocity, total and stomatal fluxes of ozone on 23 July 1998 at 12 UTC. Results correspond to moderate soil wetness conditions.

dependency on local ozone concentrations is shown during the daytime, where high ozone concentrations are obtained in the region to the southeast of the city of Budapest due to the formation of a plume from the city's emissions. Slightly higher ozone fluxes are predicted in this region. In the city, the ozone concentration is much lower due to the high local NO emission and the reaction of NO with ozone to form NO_2. In this region, slightly lower ozone fluxes are observed. The differences in ozone fluxes due to ozone concentrations are not, however, as significant as those due to changes in soil water content.

For higher soil wetness conditions a much greater spatial variability in deposition velocity and ozone flux than for low soil moisture conditions is seen. The soil wetness stress for deposition is practically negligible for wet soil conditions, and therefore ozone deposition is mostly governed by atmospheric state variables (temperature, relative humidity, etc.) and surface characteristics (albedo, roughness length, etc.), which are highly spatially variable. Again in this case, although there is clearly some influence of local ozone concentrations on ozone fluxes, other factors are also extremely significant.

4. Conclusions

A chemical transport model and a dry-deposition model were coupled for the purpose of simulating ozone fluxes over Hungary. Flux calculations without using a transport model are less precise, because of the inaccurately known spatial distribution of ozone concentrations estimated from measurements at Hungarian monitoring stations. At the same time, the spatial distribution of ozone concentration is shown to be a less accurate measure of effective ozone load than the spatial distribution of ozone flux. This flux is determined by the dry-deposition velocity of ozone, which has been estimated for different surface types within the deposition model.

The main results from the simulation of the selected scenario can be summarised as follows. In Hungary, as a

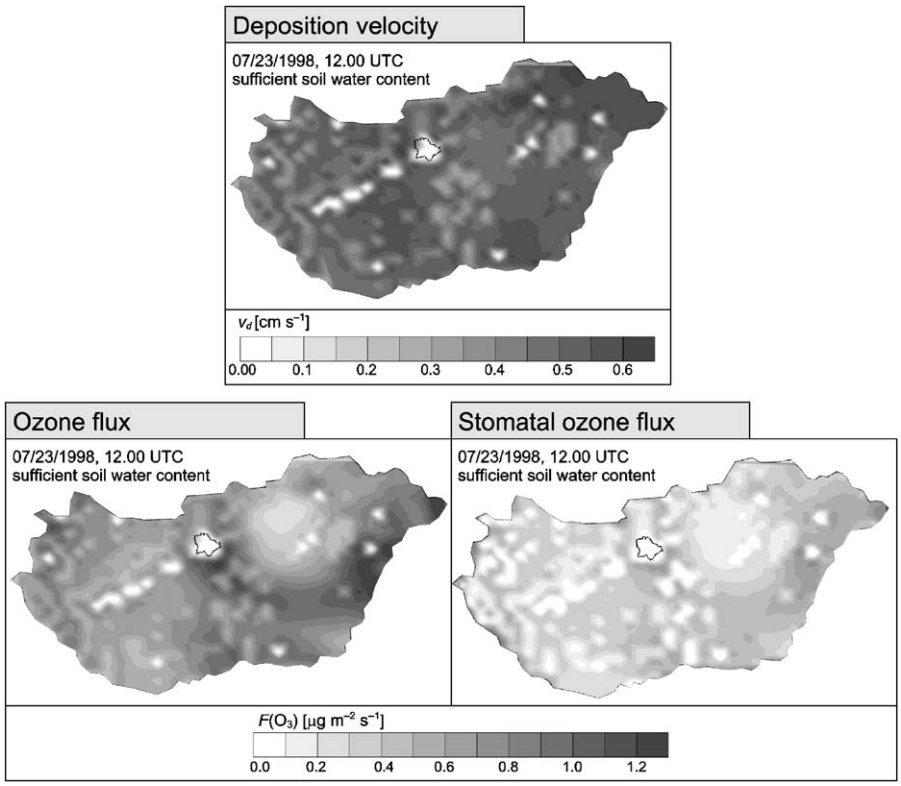

Fig. 8. Calculated dry-deposition velocity, total and stomatal fluxes of ozone on 23 July 1998 at 12 UTC. Results correspond to sufficient soil wetness conditions.

consequence of continental climatic conditions, the dry-deposition velocity of ozone depends on the soil water content during the daytime, when stomatal deposition is dominant. For high soil water contents, deposition is also influenced by atmospheric and surface characteristics and can be highly spatially variable. At night, the much smaller ozone fluxes are predominantly driven by the ozone concentration, which is independent of soil wetness conditions. Under such conditions the rather uniform resulting deposition velocity results in the magnitude of the flux being more dependent on the ozone concentration.

Consequently, the results from this study indicate that the spatial distribution of the ozone load to vegetation should be estimated by coupling high-resolution reactive transport and deposition models. Results obtained from such calculations are likely to give a more accurate measure of environmental damage than the AOT40 value and therefore provide more effective measures for characterising tropospheric ozone damage due to photochemical air pollution.

The combined model was tested on a sunny, summer day for different soil wetness conditions. The reliability of the results is determined by both the goodness of the model and the accuracy of input parameters. Parameterisation of some effects has to be implemented and reanalysed based on field measurements. There are also uncertainties in input parameters to the model such as emission rates, atmospheric forcing parameters, the soil database and land-use map. For instance, in this study only dominant soil texture and land-use are applied within each grid cell. In future work this could be improved using weighted averages. In this study, prescribed θ values have been used in order to carry out a sensitivity analysis and highlight the important effects. The development of a predictive model in the future would require the use of simulated θ values describing real conditions as well as possible. It is planned to couple the model with the ALADIN meso-scale limited area numerical weather prediction model to estimate ozone deposition over Hungary for routine application.

Table 3
Comparison of observed and modelled dry-deposition velocities

Surface	Summer observations				Model calculation for Hungary Date: 23 July 1998		
	Mean	Range	Reference	Condition	Mean	Range	Condition
Grass	0.20	0.05–0.2	Padro (1996)	Whole day	0.13	0.05–0.20	(1)
	0.24		Meyers et al. (1998)	Daytime	0.30	0.27–0.32	(2)
	0.34	0.15–0.53	Zhang et al. (2002)	Whole day	0.43	0.41–0.46	(3)
					0.53	0.49–0.57	(4)
Agricultural land	0.42	0.2–0.7	Baldocchi et al. (1987)—corn	Daytime	0.15	0.05–0.30	(1)
	0.32		Meyers et al. (1998)—corn	Whole day	0.33	0.22–0.35	(2)
					0.45	0.27–0.49	(3)
					0.56	0.31–0.62	(4)
Orchard, vineyard		0.3–0.5	Walton et al. (1997)—orchard	Daytime	0.13	0.05–0.18	(1)
		0.05–0.2		Night-time	0.21	0.20–0.22	(2)
	0.33	0.15–0.51	Zhang et al. (2002)—vineyard	Whole day	0.38	0.33–0.45	(3)
	0.30		Zhang et al. (1996)—vineyard	Whole day	0.54	0.46–0.65	(4)
Deciduous forest	0.67	0.22–1.12	Zhang et al. (2002)	Whole day	0.13	0.06–0.30	(1)
		0.19–0.83	Meyers and Baldocchi (1988)	Daytime	0.34	0.31–0.35	(2)
	0.67		Zhang et al. (1996)	Whole day	0.39	0.32–0.51	(3)
					0.45	0.32–0.65	(4)
Mixed Forest	0.50	0.14–0.86	Zhang et al. (2002)	Whole day	0.11	0.07–0.13	(1)
					0.34	0.33–0.35	(2)
					0.37	0.34–0.38	(3)
					0.40	0.34–0.44	(4)
Lake		0.004–0.04	Wesely et al. (1981)		0.03	0.02–0.03	(1)
					0.04		(2)–(3)–(4)

Conditions: (1) 00 UTC; (2) 12 UTC, insufficient soil water content; (3) 12 UTC moderate soil water content; (4) 12 UTC sufficient soil water content.

Acknowledgements

The authors acknowledge the support of OTKA grant DO48673, T043770, F047242, OMFB grant 00585/2003 (IKTA5-137), UK-Hungarian cooperation grant GB50/98 and the Békésy György Fellowship. The authors wish to thank M. Berzins (University of Leeds), J. Györffy, T. Perger (Eötvös Loránd University, Budapest), A. Horányi, G. Radnóti (Hungarian Meteorological Service).

References

Ács, F., 2003. On the relationship between the spatial variability of soil properties and transpiration. Időjárás 107, 257–272.

Ács, F., Szász, G., 2002. Characteristics of microscale evapotranspiration: a comparative analysis. Theoretical and Applied Climatology 73, 189–205.

Azzi, M., Johnson, G.J., Cope, M., 1992. An introduction to the generic reaction set photochemical smog mechanism. Proceedings of the 11th Clean Air Conference Fourth Regional IUAPPA Conference, Brisbane, Australia, pp. 451–462.

Baldocchi, D.D., Hicks, B.B., Camara, P., 1987. A canopy stomatal resistance model for gaseous deposition to vegetated canopies. Atmospheric Environment 21, 91–101.

Berzins, M., Ware, J., 1995. Positive cell-centered finite volume discretization methods for hyperbolic equations on irregular meshes. Applied Numerical Mathematics 16, 417–438.

Berzins, M., Dew, P.M., Furzeland, R.M., 1989. Developing software for time-dependent problems using the method of lines and differential algebraic integrators. Applied Numerical Mathematics 5, 375–390.

Brook, J.R., Zhang, L., Di-Giovanni, F., Padro, J., 1999. Description and evaluation of a model of deposition velocities for routine estimates of air pollutant dry deposition over North America. Part I: model development. Atmospheric Environment 33, 5037–5051.

De Santis, F., 1999. New directions: will a new European vegetation ozone standard be fair to all European countries? Atmospheric Environment 33, 3873–3874.

Emberson, L.D., Simpson, D., Tuovinen, J-P., Ashmore, M.R. Cambridge, H.M., 2000a. Towards a model of ozone deposition and stomatal uptake over Europe. EMEP MSC-W Note 6/00.

Emberson, L.D., Ashmore, M.R., Cambridge, H.M., Simpson, D., Touvinen, J.-P., 2000b. Modelling stomatal ozone flux across Europe. Atmospheric Pollution 109, 403–413.

Fuhrer, J., Skärby, L., Ashmore, M.R., 1997. Critical levels for ozone effects on vegetation in Europe. Environmental Pollution 97, 91–106.

Grünhage, L., Haenel, H.-D., 1997. PLATIN (PLant-ATmosphere INteraction) I: a model of plant-atmosphere interaction for estimating absorbed doses of gaseous air pollutants. Environmental Pollution 98, 37–50.

Hart, G., Tomlin, A., Smith, J., Berzins, M., 1998. Multi-scale atmospheric dispersion modelling by use of adaptive gridding techniques. Environmental Monitoring and Assessment 52, 225–238.

Havasi, A., Zlatev, Z., 2002. Trends of Hungarian air pollution levels on a long time-scale. Atmospheric Environment 36, 4145–4156.

Hicks, B.B., Baldocchi, D.D., Meyers, T.P., Hosker, R.P., Matt, D.R., 1987. A preliminary multiple resistance routine for deriving dry deposition velocities from measured quantities. Water, Air and Soil Pollution 36, 311–330.

Hjellbrekke, A-G., Solberg, S., 2002. Ozone measurments 2000. EMEP/CCC-Report 5/2002.

Horányi, A., Ihász, I., Radnóti, G., 1996. ARPEGE/ALADIN: a numerical Weather prediction model for Central-Europe with the participation of the Hungarian Meteorological Service. Issue Series Title: Időjárás 100, 277–301.

Jarvis, P.G., 1976. The interpretation of the variations in leaf water potential and stomatal conductance found in canopies in the field. Philosophical Transactions of the Royal Society of London Series B 273, 593–610.

Jonson, J.E., Sundet, J.K., Tarrasón, L., 2001. Model calculations of present and future levels of ozone and ozone precursors with a global and a regional model. Atmospheric Environment 35, 525–537.

Kärenlampi, L., Skärby, L. (Eds.), 1996. Critical levels for ozone in Europe: Testing and finalizing the concepts. UNECE Workshop Report. University of Kuopio, Department of Ecology and Environmental Science, Kuopio, Finland.

Klemm, O., Mangold, A., 2001. Ozone deposition at a forest site in the Bavaria. Water, Air and Soil Pollution: Focus 1, 223–232.

Kramm, G., Dlugi, R., Dollard, G.J., Foken, Th., Mölders, N., Müller, H., Seiler, W., Sievering, H., 1995. On the dry deposition of ozone and reactive nitrogen species. Atmospheric Environment 29, 3209–3231.

Krupa, S.V., Manning, W.J., 1988. Atmospheric ozone: formation and effects on vegetation. Environmental Pollution 50, 101–137.

Lagzi, I., Tomlin, A.S., Turányi, T., Haszpra, L., Mészáros, R., Berzins, M., 2001. The simulation of photochemical smog episodes in Hungary and Central Europe using adaptive gridding models. Lecture Notes in Computer Science 2074, 67–77.

Lagzi, I., Tomlin, A.S., Turányi, T., Haszpra, L., Mészáros, R., Berzins, M., 2002. Modelling photochemical air pollution in Hungary using an adaptive grid model. In: Sportisse, S. (Ed.), Air Pollution Modelling and Simulation. Springer, Berlin, pp. 264–273.

Lagzi, I., Kármán, D., Turányi, T., Tomlin, A.S., Haszpra, L., 2004. Simulation of the dispersion of nuclear contamination using an adaptive Eulerian grid model. Journal Environmental Radioactivity 75, 59–82.

Meyers, T.P., Finkelstein, P., Clarke, J., Ellestad, T.G., Sims, P.F., 1998. A multilayer model for inferring dry deposition using standard meteorological measurements. Journal of Geophysical Research 103, 22645–22661.

Mintz, Y., Walker, G.K., 1993. Global fields of soil moisture and land surface evapotranspiration derived from observed precipitation and surface air temperature. Journal of Applied Meteorology 32, 1305–1334.

Padro, J., 1996. Summary of ozone dry deposition velocity measurements and model estimates over vineyard, cotton, grass and desciduous forest in summer. Atmospheric Environment 30, 2363–2369.

Padro, J., den Hartog, G., Neumann, H.H., 1991. An investigation of the ADOM dry deposition module using summertime O_3 measurements above a deciduous forest. Atmospheric Environment 30, 339–345.

Padro, J., Zhang, L., Massman, W.J., 1998. An analysis of mesurements and modelling of air-surface exchange of $NO–NO_2–O_3$ over grass. Atmospheric Environment 32, 1167–1177.

Sofiev, M., Tuovinen, J-P., 2001. Factors determining the robustness of AOT40 and other ozone exposure indices. Atmospheric Environment 35, 3521–3528.

Tomlin, A., Berzins, M., Ware, J., Smith, J., Pilling, M.J., 1997. On the use adaptive gridding methods for modelling chemical transport from multi-scale sources. Atmospheric Environment 31, 2945–2959.

Tuovinen, J-P., 2000. Assessing vegetation exposure to ozone: properties of the AOT40 index and modifications by deposition modelling. Environmental Pollution 109, 361–372.

Van Loon, M., 1996. Numerical methods in smog prediction. Ph.D. Thesis, GWI Amsterdam.

Várallyay, Gy., Szűcs, L., Murányi, A., Rajkai, K., Zilahy, P., 1980. Map of soil factors determining the agro-ecological potential of Hungary (1:100 000) II. Agrokémia és Talajtan 29, 35–76 (in Hungarian).

Walmsley, J.L., Wesely, M.L., 1996. Modification of coded parameterizations of surface resistances to gaseous dry deposition (Technical note). Atmospheric Environment 30, 1181–1188.

Walton, S., Gallagher, M.W., Choularton, T.W., Duyzer, J., 1997. Ozone and NO_2 exchange to fruit orchards. Atmospheric Environment 31, 2767–2776.

Wesely, M.L., 1989. Parameterization of surface resistances to gaseous dry deposition in regional-scale numerical models. Atmospheric Environment 23, 1293–1304.

Wesely, M.L., Cook, D.R., Williams, R.M., 1981. Field measurements of small ozone fluxes to snow, wet bare soil and lake water. Boundary Layer Meteorology 20, 459–471.

Zhang, L., Padro, J., Walmsley, J.L., 1996. A multi-layer model vs. single-layer models and observed O_3 dry deposition velocities. Atmospheric Environment 25, 1689–1704.

Zhang, L., Moran, M.D., Brook, J.R., 2001. A comparison of models to estimate in-canopy photosynthetically active radiation and their influence on canopy stomatal resistance. Atmospheric Environment 35, 4463–4470.

Zhang, L., Moran, M.D., Makar, P.A., Brook, R., Gong, S., 2002. Modelling gaseous dry deposition in AURAMS: a unified regional air-quality modelling system. Atmospheric Environment 36, 537–560.